A framework for predicting global silicate weathering and CO_2 drawdown rates over geologic time-scales

George E. Hilley[a,1] and Stephen Porder[b]

[a]Department of Geological and Environmental Sciences, Stanford University, Stanford, CA 94062; and [b]Department of Ecology and Evolutionary Biology, Brown University, Providence, RI 02912

Global silicate weathering drives long-time-scale fluctuations in atmospheric CO_2. While tectonics, climate, and rock-type influence silicate weathering, it is unclear how these factors combine to drive global rates. Here, we explore whether local erosion rates, GCM-derived dust fluxes, temperature, and water balance can capture global variation in silicate weathering. Our spatially explicit approach predicts 1.9–4.6×10^{13} mols of Si weathered globally per year, within a factor of 4–10 of estimates of global silicate fluxes derived from riverine measurements. Similarly, our watershed-based estimates are within a factor of 4–18 (mean of 5.3) of the silica fluxes measured in the world's ten largest rivers. Eighty percent of total global silicate weathering product traveling as dissolved load occurs within a narrow range (0.01–0.5 mm/year) of erosion rates. Assuming each mol of Mg or Ca reacts with 1 mol of CO_2, 1.5–3.3×10^8 tons/year of CO_2 is consumed by silicate weathering, consistent with previously published estimates. Approximately 50% of this drawdown occurs in the world's active mountain belts, emphasizing the importance of tectonic regulation of global climate over geologic timescales.

chemical weathering | geologic carbon cycle | landscape development | riverine chemical fluxes

Silicate weathering is the most important regulator of atmospheric CO_2 over million year timescales (1). While quantitative estimates of modern global silicate weathering exist (2–4), they are based on the summation of river fluxes and leave several questions unanswered: i) What are the watershed-scale controls on weathering rates for rivers that pass through areas of vastly different topography, such as those whose headwaters source mountainous regions but flow through stable cratonic areas downstream? ii) Where in a basin does most weathering occur? and, iii) Can we quantify the relationship between likely controls and weathering rate? For example, can we move from an observation that erosion rate covaries with river silica fluxes (5) to a quantitative prediction of the flux coming out a basin based on factors such as erosion rate and climate?

To develop such a prediction, we need to understand and quantify the fundamental controls on the rates of silicate weathering. In the most general sense, the rate of weathering is a function of the supply of weatherable substrate and the reaction kinetics of its constituent minerals. Mineral supply over hundreds of thousands to millions of years is regulated by the disaggregation of bedrock as Earth's surface is eroded (6) and the import of exogenous materials as dust (7, 8). However, the mineral reaction kinetics depend on myriad factors—ranging from irregularities in the mineral lattice to secondary mineral formation to watershed hydrologic flowpaths—that are difficult to determine for a watershed, let alone for the globe. These complexities have prevented laboratory observations from being applied to larger spatial scales using a strictly process-based approach to weathering—although recent progress has been made in linking lab and field-based estimates of basalt weathering (9, 10). Given our current lack of knowledge regarding the specific weathering processes, their rates, and how they interact with one another, a comprehensive, process-based model of silicate weathering that can predict continental-scale, regional-scale, or even catchment-scale silicate weathering fluxes seems unlikely to emerge in the near future.

Despite these complexities, several empirical observations suggest that silicate-weathering fluxes vary somewhat systematically at regional scales. For example, stable cratons that contain ancient and penetratively weathered materials produce lower Si-fluxes than areas in which fresh, unweathered bedrock is abundant (11, 12). Likewise, weathering of material in semiarid or arid environments is often limited, and these weathering products are typically reprecipitated within soils before they reach regional rivers and thus are not likely to participate appreciably in global elemental cycling over geologic timescales (13). In contrast, young weathering zones with ample fresh bedrock and humid zones with high infiltration rates tend to produce larger weathering fluxes than their older, dryer counterparts (13).

These observations make intuitive sense, but it is unclear how to use them to understand the regional-scale controls on chemical weathering and predict silicate-weathering rates. To this end, we parameterize silicate weathering over regional scales in a way that captures the essence of the aforementioned empirical observations while simplifying the numerous complexities of mineral, soil, and watershed-scale weathering processes into a tractable form. We construct this model in the spirit of global geologic carbon cycle models (1, 14–16) to present a conceptually and numerically simple model of the processes of mineral supply and chemical reactions and populate the model with spatially explicit geolomorphic and climatic data. Here we present the first prediction of silicate weathering fluxes at the global scale using a range of geographically explicit parameters at high spatial resolution ($0.5 \times 0.5°$), integrating some existing watershed-scale weathering components of this model (12, 17, 18) with an understanding of weathering zone propagation rates, climatic variability, and the role of exogenous material as a substrate for chemical weathering.

Results

Our formulation considers the effects of four parameters on silicate weathering: i) the effects of mineral supply as bedrock is weathered to saprolite and dust is mixed into the soil, ii) the time-scale of reactions of individual mineral phases in relation to the residence time of rock in the weathering zone, iii) the effect of precipitation, since weathering is markedly diminished in areas where evaporation exceeds precipitation (19), and iv) the

GEOLOGY

effect of freezing temperatures, since weathering fluxes decrease markedly when the ground is frozen (20).

The supply rate of bedrock-derived minerals made available to the weathering process is proportional to the downward propagation rate of the weathering zone into fresh rock (21), which we posit is dynamically coupled to the rate at which erosion removes material from the surface. We argue this must indeed be the case—a long-term imbalance in these rates would lead to either the ubiquitous exposure of bare, unweathered rock or the development of an infinitely thick weathering zone. Erosion rate and weathering zone thickness together determine how long minerals remain exposed to weathering before removal and transport, and it has been shown that the thickness of the weathering zone is itself related to the erosion rate (22, 23), climate (13), and likely several other geologic and biologic factors. Unfortunately, quantitative characterization of this relationship on broad spatial scales is intractably difficult, since weathering zone thickness is quite variable and rarely measured at more than a few happenstance sampling points. In addition, there is no theory that details the functional relationship between erosion rates and soil thicknesses across a broad range of these values. However, a logarithmic relationship between soil thickness and erosion rate for steadily eroding landscapes has been verified by field observations (23), and so, in the absence of more data, we assume this relationship is representative of weathering-zone thickness as well. Given the limited support for this assumption, it is necessary to bracket a plausible relationship between erosion rate and weathering zone thickness, and to assess the sensitivity of our results to this oversimplification. We assume that at high erosion rates (> 2 mm/year), materials are only shallowly weathered (0.5 m), while at low erosion rates (approximately 10^{-6} mm/year), weathering extends to roughly 20–100 m (the shallow weathering zone scenario [SWZ] and deep weathering zone scenario [DWZ], respectively; [supporting information (SI)]), based on estimates in slowly eroding tectonically inactive regions. It is unlikely we will ever have enough data to accurately describe this relationship across the globe, and while the small available sample size of well-studied sites introduces considerable uncertainty, the large range of weathering zone thicknesses considered for each erosion rate represents generous bounds on the current state of knowledge as to how these two factors are related.

When erosion rates are constant over time (assumed in the remainder of this analysis) weathering zone thickness sets the time over which a particular mineral weathers before it is removed by erosional processes and ultimately buried in the deep ocean. We calculate erosion rates based on topographic relief (24) and use the relationships described above to bound estimates of weathering zone thickness. These estimates of erosion rates are averaged over $0.5° \times 0.5°$ regions to match the resolution of the rest of our datasets. As a result, our peak averaged erosion rates are generally slower than those measured over small areas in the field, but are consistent with this scale of spatial averaging (25).

By assigning an erosion rate value to each point on Earth's surface, we assume that all points on Earth's surface are lowered over time, which neglects the reality that deposition characterizes significant areas of Earth's surface where weathering may be important. However, no methods currently exist that may be used to estimate deposition rates over spatial scales similar to those used here to bound erosion rates. Should global-scale estimates of deposition rate become available, our model formulation could be modified to accommodate this new information. In the present study, we simply assume that weathering fluxes can be adequately characterized in the low-relief depositional areas of the world by instead using the low erosion rate values predicted by our topographically derived estimates. This causes us to underestimate the contribution of weathering from depositional areas that are supplied with ample fresh minerals (such as the Bengali plain) and overestimate weathering in those depositional areas supplied with pervasively weathered materials (such as local basins draining saprolites of the Amazon basin).

In addition to bedrock supply from below, dust may supply fresh minerals to the upper portion of the weathering zone and thus may enhance weathering rates. Field studies suggest that dust is mixed mostly into the uppermost portion of the weathering zone (26), and we allow this mixing length to vary in our model. However, as we show below, the total inputs from dust weathering are $<10\%$ of the total weathering budget, even for the maximum mixing length (and dust residence time). Because the factors controlling this mixing length (rooting depth, tree throw depth, burrowing animals, etc.) are poorly quantified and the model is generally insensitive to its choice, we equate the mixing zone with the entire weathering zone thickness for the remainder of our study, which yields a maximum bound for dust contribution to weathering fluxes. We use dust deposition rates from NCAR's CCSM-3 GCM (27). As dust rates are known to vary between glacial-interglacial cycles, we considered dust deposition rates for modern (hereafter MOD) and last glacial maximum (hereafter LGM) scenarios (27). For simplicity, we assume that bedrock and dust have the composition of average continental crust (28), and that this composition is assumed to be everywhere spatially uniform. This may cause us to underestimate the influence of mafic-rich island arcs on global silicate weathering (hereafter Si_{tot}), while overestimating the contribution of carbonates and quartz-rich sandstones (29, 30). However, given the paucity of published mafic mineral weathering rates, we view inclusion of detailed variation in composition as an overparameterization for a study at the global scale.

We simplify the processes of silicate mineral dissolution by regarding the rate of change in molar concentration of a particular mineral phase (in mols m^{-3} s^{-1}) as linearly proportional to the its instantaneous molar concentration (mols m^{-3}) and reactive surface area (A) times a kinetic rate constant (k) for each mineral. While such a treatment represents a gross oversimplification of the chemical weathering processes, it captures the observation that reaction rates decrease with mineral abundance over a specific time-scale that varies between different minerals. Dissolution rates for substrate minerals are based on field-calibrated weathering constants (17) and are consistent with global estimates for these values (21).

Finally, climate enters our analysis by way of monthly temperature (T), precipitation (P), and potential evapotranspiration (PEt). We weight regions according to the fraction of the year that each experience subzero temperatures because chemical weathering effectively ceases below 0 °C (20). Similarly, where PEt $\gg$ P, weathering rates decline by at least an order of magnitude (13, 19). However, the timescale over which weathering responds to water availability is on the order of 10^3-10^4 years (13) and as a result, modern P and PEt distributions offer only a rough guide with which to determine regions with negligible weathering rates. To account for this uncertainty, we explored two scenarios, one in which weathering does not occur in regions where P $<$ PEt (hereafter 0 P-Et) and another in which weathering only ceases when P is 500 mm/year $<$ PEt (hereafter 500 P-Et). Admittedly, this treatment is an oversimplification, albeit one that is not unreasonable in light of the limited long time-scale climate data available (13). We choose this oversimplification rather than creating more complicated scenarios relating weathering rates to P-Et for which there is little empirical support.

Given these assumptions, we calculate silicate-weathering fluxes for each $0.5° \times 0.5°$ region as:

Table 1. Si, Ca, Mg weathering and CO_2 drawdown for MOD-LGM-P-Et 0 scenario

	MOD Discharge	LGM Discharge	Percent by Region for MOD Dust Fluxes							
	10^{12} mols/year	10^{12} mols/year	Andes	Central America	Caucases	Europe	Himalayas	Asia Pacific	Amazon	Other
Si	19–46	23–71	5.3–6.8	1.2–1.7	0.7–3.1	3.8–4.8	16–20	7.4–12.8	3.5–6.9	50–59
Ca	1.8–4.5	2.3–7.0	4.0–6.7	1.1–1.7	0.4–3.1	3.5–4.7	14–18	7.3–13.0	3.4–7.7	51–63
Mg	1.6–2.9	2.1–4.2	8.4–9.2	1.4–1.8	1.3–3.5	4.6–5.9	21–27	7.8–13.2	2.4–3.8	44–46
CO_2	3.4–7.5	4.4–11.2	6.3–7.5	1.3–1.7	0.9–3.2	4.0–5.1	17–22	7.6–13.0	4.6–5.9	48–55

$$F_w^i = W_{pet}W_t r^i \left(\varepsilon q_o^i \left(1 - \exp\left(-k^i A^i \frac{H}{\varepsilon}\right)\right) \right.$$

$$\left. + F_{dust}^i \left(1 - \frac{\varepsilon}{hk^i A^i}\left(1 - \exp\left(-k^i A^i \frac{h}{\varepsilon}\right)\right)\right)\right)$$

where F_w^i is the flux of a given mineral phase (mol m^{-2} s^{-1}), r^i is the stochiometric ratio of elements of interest in each mineral phase, ε is erosion rate (m s^{-1}), H is the weathering zone thickness (m), h is the mixing depth (m; herein set equal to H), q_o^i is the molar concentration of each mineral phase (mol m^{-3}), k^i (mol m^{-2} s^{-1}) and A^i (m^2 mol^{-1}) are the kinetic rate constants and surface areas of each phase, F_{dust}^i is the dust flux (mol m^{-2} s^{-1}), W_t is the fraction of the year that each pixel experienced temperatures greater than 0 °C, and $W_{pet} = 0$ if P < PEt and P-500 < PEt, for scenarios 0 P-Et and 500 P-Et, respectively, but = 1 otherwise. Weathering rates were calculated by integrating these fluxes over each 0.5° × 0.5° region and adjusting for area changes with latitude. Thus, our model expresses the weathering flux in terms of the supply rates of minerals from dust and bedrock (F_{dust}^i and $q_o^i\varepsilon$, respectively), the time over which dust or rock resides in the weathering zone (h/ε or H/ε, respectively), the reaction timescale ($k_i^{-1}A_i^{-1}$), and a rough depiction of how these kinetics may be affected by a negative water balance (W_{pet}) and subzero temperatures (W_t).

Even though our model has a limited number of parameters and oversimplifies the weathering process, our estimate of Si$_{tot}$ ranges from 1.9–4.6 × 10^{13} mols/year (Table 1), within a factor of 4–10 of values extrapolated from river chemistry and discharge (2–4). Our global estimates of Si$_{tot}$ tend to be systematically higher than those observed—this likely reflects the fact that all silica release from primary minerals contributes to the riverine budget in our model. In reality, the formation of secondary minerals likely absorbs a fraction of Si$_{tot}$, depending on the specific mineral stoichiometry. This would cause our model to overestimate silicate-weathering fluxes, which indeed occurs in our model predictions. Nonetheless, the fact that our predicted MOD values of Si$_{tot}$ show general agreement with observed values is encouraging given the considerable uncertainty associated with both our model parameters and empirical observations (discussed below).

According to our model, the major sources for silicate weathering are the Himalayas and Southeast Asia (Fig. 1), which contribute approximately 20% to the global total. However, this may be an overestimate, as the mountains of Southeast Asia that contribute substantively to silicate weathering contain a disproportionate area of carbonates, as opposed to the continental crust composition assumed in our model (31). Silicate weathering fluxes are also high within other active mountain ranges (particularly the Andes), but low relief regions still contribute substantially to the total weathering budget because of their large area (Table 1). In some of these low-relief areas, the exposure of sediments that may be depleted in primary silicate minerals, such as shales (31), may cause us to overestimate the contribution of these areas to Si$_{tot}$. Using modern dust fluxes, dust weathering accounts for <10% in the scenarios described above. Because dust is allowed to mix throughout the entire weathering zone in our model, our predicted residence times over which dust is allowed to weather are likely unrealistically large. Coupled with the fact that dust may have undergone significant weathering before its ultimate deposition, we speculate that even the low dust contribution that we infer is likely an overestimate of the true contribution that dust makes to the overall weathering budget. The Si$_{tot}$ and the fraction contributed
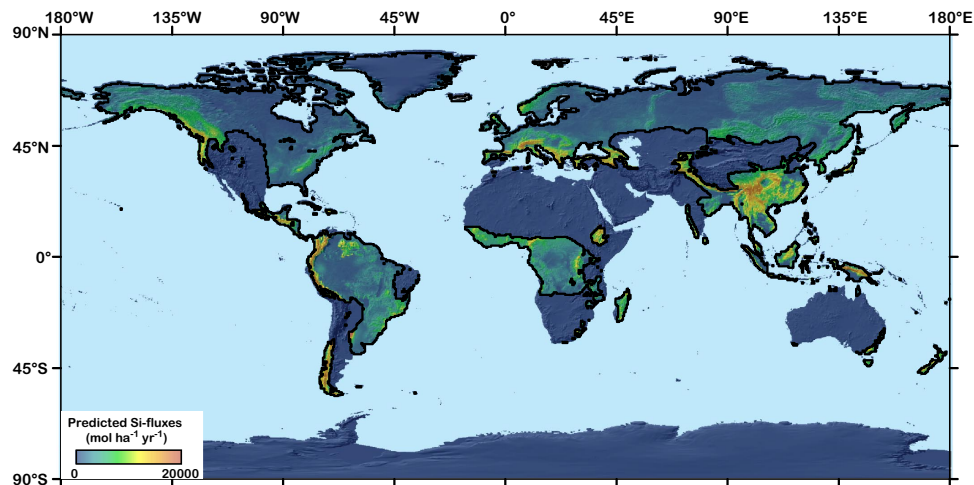
Fig. 1. Spatially explicit predicted Si fluxes (mol·ha^{-1}·year^{-1}) for each 0.5° × 0.5° region (excluding Antarctica). The black line highlights the regions where P > PEt, all other regions are assumed not to contribute to silicate weathering. The scenario shown here is based on modern dust fluxes and our deep weathering zone scenario (DWZ). LGM and SWZ scenarios, evaluated for both P-Et 0 and P-Et 500 are available in SI.
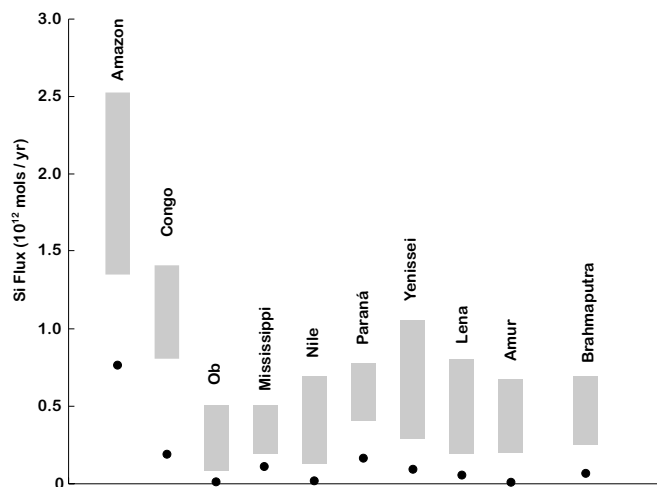
Fig. 2. Comparison between observed (solid dots) and modeled (gray fields) silicate-weathering rates for large river basins of the world. Observed weathering rates calculated from ref. 3. Modeled rates were performed for the DWZ and SWZ models for only the MOD scenario. The extent of the gray fields denotes the variation in silicate weathering rates that arises from our use of the DWZ versus SWZ model.

by dust increases by no more than 120–160% of modern values under the LGM scenario (Table 1) as a result of additional dust deposition and weathering.

We can determine how well regional Si discharges are predicted by our approach by comparing it to modern silica fluxes in specific regional to continental scale watersheds. Given our assumption that Earth's surface is of uniform lithology, we expect that only the world's largest catchments approach a scale over which local variations in rock type may average to produce a mineralogy representative of average continental crust. In South America, the proportion of Si_{tot} derived from the upland Andes is roughly equal to that from the Amazon lowlands, and so Andean weathering accounts for <50% of the observed Si flux from the Amazon River, in agreement with river-based estimates (32). A comparison of our estimates with empirical observations from the world's ten largest rivers (Fig. 2) indicates that our approach produces large catchment weathering fluxes that are also broadly consistent with the limited riverine Si fluxes that have been inferred based on field measurements. It is also worth noting that in humid, low erosion areas such as central Africa and eastern South America, our model indicates that dust rather than bedrock weathering is capable of providing the bulk of weatherable substrate (SI), although we likely overestimate the dust-derived contribution to weathering in these areas due to the assumption of deep mixing of dust in our model. The effect of the moisture balance on Si_{tot} is illustrated by the $\approx 1.7\times$ difference between the 0 P-Et and 500 P-Et scenarios (SI).

While our model predicts large spatial variability in Si derived from silicate weathering fluxes (Si_w), 80% of Si_{tot} is produced in regions eroding between 0.01–0.5 mm/year (Fig. 3), approximately 65% of Earth's weatherable surface (SI). This result is perhaps most interesting in light of two fundamental limiting controls on Si_w, mineral supply and chemical dissolution rates (17). In areas with shallow weathering and rapid erosion, mineral supply is abundant and Si_w is controlled by the rate of mineral dissolution. Where materials are deeply weathered and erosion is slow, chemical weathering proceeds to near completion, and Si_w is instead limited by mineral supply. Our data indicate that the majority of active mountain belts lie between these two extremes, where dissolution and mineral supply are sufficient to produce the highest values of Si_w. In addition, the uniform
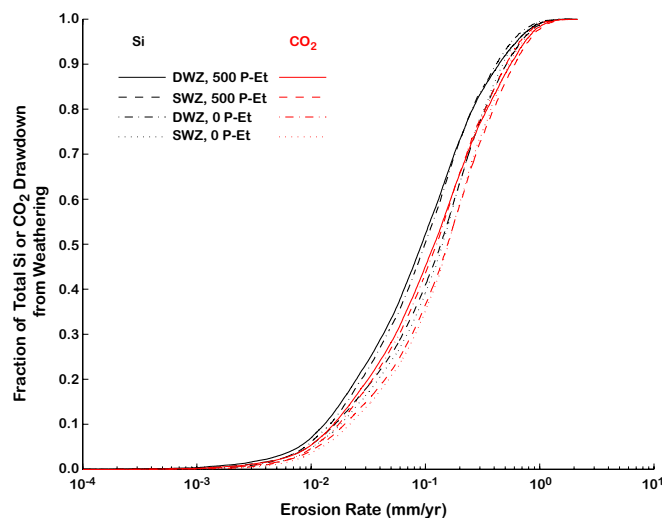

Fig. 3. Fraction of Si_{tot} and CO_2 consumption that occurs at given weathering rates under our two weathering zone and precipitation scenarios. Note that the results are relatively insensitive to shifts in weathering zone thickness or between the P-Et 0 and P-Et 500 scenarios. A narrow range of erosion rates (relative to the global range predicted by ref. 23) produces a large portion of Si_{tot} and CO_2 consumption according to our model, indicating that conditions in which supply rates are relatively high and rock resides for a substantial amount of time in the weathering zone produce a disproportionate fraction of global silicate weathering.

mineralogic composition we assume may cause us to underestimate the importance of rapidly uplifting areas relative to slowly eroding stable cratons due to the fact that cover rocks such as shales that may be relatively depleted in primary silicate minerals are generally found in low-lying, low relief areas (31). Thus, the actively uplifting crystalline core of many orogens may play a role even stronger than our model predicts.

Discussion

The approach taken here strives to simplify and parameterize the factors that control silicate weathering in a form that may be used to predict weathering fluxes based on quantities that can be inferred at regional and global scales. As such, it is subject to the same drawbacks of any global or geologic-time-scale model (1, 15, 16), since it surely misses many of the subtleties that drive regional and local differences. Nevertheless, these types of models have proven extremely valuable in framing our ideas about global-scale processes through geologic time.

Similarly, there are several oversimplifications in our model that may lead to incorrect predictions at the local and regional scale (see SI for further discussion). For example, by assuming a uniform granitic lithology, we systematically underestimate the weathering flux from mafic-rich provinces, and overestimate the importance of lithologies poor in primary silicate minerals such as carbonates and mature sandstones. However, the river flux estimates to which we compare our model results are also subject to considerable and almost universally unreported uncertainty, since large rivers inevitably drain both mountainous and lowland regions where recent elemental fluxes may have been substantially altered by human activity (33), as well as the fact that detailed time-series of riverine Si concentration and corresponding discharges that may be used to assess measurement uncertainties are rarely collected. The agreement between our approach and empirical weathering estimates for both specific large catchments and global estimates of Si_{tot} is encouraging and may suggest that such a simplification may have captured the essence, if not the specific processes, of silicate weathering in a way that

Hilley and Porder

may be used to predict both modern, and perhaps ancient silicate-weathering fluxes.

We have focused our discussion on Si, but the connection between silicate weathering and CO_2 drawdown lies in the release of Ca and Mg stored in silicate minerals (34). We calculated Si_{tot}-driven CO_2 drawdown by incorporating the mineral stochiometries of average continental crust and assuming that 1 mol of CO_2 is consumed for every mol of Ca or Mg released by weathering. As such, these calculations place an upper bound on CO_2 drawdown from silicate weathering. Globally, Si_{tot} is associated with the consumption of $1.5–3.3 \times 10^8$ tons CO_2/yr under modern dust fluxes (Table 1). Published CO_2

drawdown rates based on extrapolations of measured river chemistry are between $5.1–5.5 \times 10^8$ tons CO_2/yr (2–4), again, in close agreement with our estimates. As with Si_{tot}, approximately 20% of this drawdown occurs within mountains of the Indo-Asian collision (Table 1), which lends further support to the hypothesis that the continued uplift of the Himalayas during the late Cenozoic has played a major role in moderating Earth's climate (35).

1. Berner RA (1990) Atmospheric CO2 levels over Phanerozoic time. *Science* 249:1382–1386.
2. Berner RA, Lasaga AC, Garrels RM (1983) The carbonate-silicate geochemical cycle and its effect on atmospheric carbon dioxide over the past 100 million years. *American Journal of Science* 283:641–683.
3. Gaillardet J, Dupre B, Louvat P, Allegre C (1999) Global silicate weathering and CO2 consumption rates deduced from the chemistry of large rivers. *Chem Geol* 159:3–30.
4. Maybeck M (1987) Global chemical weathering of surficial rocks estimated from river dissolved loads. *Am J Sci* 287:401–428.
5. Stallard RF, Edmond JM (1983) Geochemistry of the Amazon 2: The influence of geology and weathering environment on the dissolved load. *J Geophys Res* 88(C14):9671–9688.
6. Riebe CS, Kirchner JW, Granger DE, Finkel RC (2001) Strong tectonic and weak climatic control of long-term chemical weathering rates. *Geology* 29:511–514.
7. Jackson ML, *et al.* (1971) Geomorphological relationships of tropospherically-derived quartz in the soils of the Hawaiian Islands. *Soil Sci Soc Am Procs* 35:515–525.
8. Muhs DR, Budahn JR (2007) Geochemical evidence for African dust inputs to soils of western Atlantic Islands: Barbados, the Bahamas, and Florida. *J Geophys Res*, 101029/2005JF 000445:002007.
9. White AF, Brantley SL (2003) The effect of time on the weathering of silicate minerals: Why do weathering rates differ in the laboratory and the field? *Chem Geol* 202:479–506.
10. Navarre-Sitchler A, Brantley SL (2007) Basalt weathering across scales. *Earth Planet Sci Lett* 261:321–334.
11. Riebe CS, Kirchner JW, Finkel RC (2004) Erosional and climatic effects on long-term chemical weathering rates in granitic landscapes spanning diverse climate regimes. *Earth Planet Sci Lett* 224:547–562.
12. West AJ, Galy A, Bickle M (2005) Tectonic and climatic controls on silicate weathering. *Earth Planet Sci Lett* 235:211–228.
13. Porder S, Hilley GE, Chadwick O.A. (2007) Chemical weathering, mass loss, and dust inputs across a climate by time matrix in the Hawaiian Islands. *Earth Planet Sci Lett* 258:414–427.
14. Berner RA (1991) A model for atmospheric CO2 over phanerozoic time. *Am J Sci* 291:339–376.
15. Caldeira K (1992) Enhances Cenozoic chemical weathering and the subduction of pelagic carbonate. *Nature* 357:578–581.
16. Kump LR (1989) Alternative modeling approaches to the geochemical cycles of carbon, sulfur, and strontium isotopes. *Am J Sci* 289:390–410.
17. Hren MT, Hilley GE, Chamberlain CP (in press) The relationship between tectonic uplift and chemical weathering rates in the Washington Cascades: Field measurements and model predictions. *Am J Sci*, 10.2475/2406.2007.2400.
18. Waldbauer JR, Chamberlain CP (2005) in *A History of Atmospheric CO2 and its Effects on Plants, Animals, and Ecosystems*, eds Cerling TE, Ehleringer JR, Dearing MD (Springer, Heidelberg), pp 166–184.
19. Chadwick OA, *et al.* (2003) The impact of climate on the biogeochemical functioning of volcanic soils. *Chem Geol* 202:195–223.
20. Riebe CS, Kirchner JW, Finkel RC (2004) Sharp decrease in long-term chemical weathering rates along an altitudinal transect. *Earth Planet Sci Lett* 218:421–434.
21. White AF, Brantley SL eds. (1995) *Chemical Weathering Rates of Silicate Minerals* (Mineralogical Society of America, Washington, D.C.).
22. Gilbert GK (1877) *Report on the Geology of the Henry Mountains* (Government Printing Office, Washington, D.C.).
23. Heimsath AM, Dietrich WE, Nishiizumi K, Finkel RC (1997) The soil production function and landscape equillibrium. *Nature* 388:358–361.
24. Montgomery DR, Brandon MT (2002) Topographic controls on erosion rates in tectonically active mountain ranges. *Earth Planet Sci Lett* 201:481–489.
25. Vance D, Bickle M, Ivy-Ochss S, Kubik P (2003) Erosion and exhumation in the Himalaya from cosmogenic isotope inventories of river sediments. *Earth Planet Sci Lett* 206:273–288.
26. Kurtz AC, Derry LA, Chadwick OA (2001) Accretion of Asian dust to Hawaiian soils: Isotopic, elemental and mineral mass balances. *Geochem Cosmochim Acta* 65:1971–1983.
27. Mahowald NM, *et al.* (2006) Change in atmospheric mineral aerosols in response to climate: Last glacial period, preindustrial, modern, and doubled carbon dioxide climates. *J Geophys Res* 101029/2005JD 006643:002006.
28. Taylor SR, McClennan SM (1985) *The Continental Crust: Its Composition and Evolution* (Blackwell Scientific, Oxford).
29. Dessert C, Dupré B, Gaillarde J, François LM, Allègre CJ (2003) Basalt weathering laws and the impact of basalt weathering on the global carbon cycle. *Chem Geol* 202:257–273.
30. Edmond JM, Palmer MR, Measures CI, Grant B, Stallard RF (1995) The fluvial geochemistry and denudation rate of the Guayana Shield in Venezuela, Columbia, and Brazil. *Geochem Cosmochim Acta* 59:3301–3325.
31. Suchet PA, Probst J-L, Ludwig W (2003) Worldwide distribution of continental rock lithology: Implications for the atmospheric/soil CO2 uptake by contienntal weathering and alkalinity river transport to the oceans. *Global Biogeochem Cycles* 17:1038.
32. Gaillardet J, Dupré B, Allègre CJ, Negrel P (1997) Chemical and physical denudation of the Amazon River Basin. *Chem Geol* 142:141–173.
33. Raymond PA, Oh N, Turner RE, Broussard W (2008) Anthropogenically enhanced fluxes of water and carbon from the Mississippi River. *Nature* 451:449–452.
34. Urey HC (1952) *The Planets, Their Origin and Development.* (Yale Univ Press, New Haven).
35. Raymo ME, Ruddiman WF (1992) Tectonic forcing of late Cenozoic climate. *Nature* 359:117–122.

GEOLOGY